

Determination and ecological risk assessment of arsenic and mercury in sediments from the Changjiang River Estuary and adjacent East China Sea

Yu'na Zhang¹, Qianwen Wang^{1*}

¹ Central Laboratory, Qingdao Agricultural University, Qingdao 266109, China

Received 15 May 2020; accepted 4 August 2020

© Chinese Society for Oceanography and Springer-Verlag GmbH Germany, part of Springer Nature 2021

Abstract

Arsenic (As) and mercury (Hg) are pollutants presented in marine environment. A process of atomic fluorescence spectrometry was proposed for the simultaneous determination of As and Hg in marine sediment samples ($n = 38$) collected from the Changjiang River Estuary and adjacent East China Sea. The proposed method used an optimized pretreatment procedure in an aqua regia–H₂O digestion system. Recoveries of As and Hg increased to 97% and 98%, respectively, with suitable precisions (2.7%–4.1%) under optimized process conditions. As and Hg were widely presented in these samples, with the ranges of content values were 2.39–8.77 μg/g for As and 48.03–410.8 ng/g for Hg. Results indicate that anthropogenic factors strongly influence the abundances of As and Hg in investigated samples. The preliminary environmental risk assessment was investigated using the geoaccumulation index (I_{geo}) and anthropogenic contribution rate (M). Findings reveal that Hg demonstrates a strong ecological risk (with average values of 1.3 and 72% for I_{geo} and M , respectively) in the sediments from the Changjiang River Estuary and adjacent East China Sea. Therefore, Hg should be considered in future investigations.

Key words: arsenic, mercury, marine sediment, spatial distributions, ecological risk

Citation: Zhang Yu'na, Wang Qianwen. 2021. Determination and ecological risk assessment of arsenic and mercury in sediments from the Changjiang River Estuary and adjacent East China Sea. Acta Oceanologica Sinica, 40(4): 32–38, doi: 10.1007/s13131-021-1772-8

1 Introduction

Rapid industrial and economic development in China has led to serious environmental pollution at some time in the past, which is cause for concern (Awasthi et al., 2018; Shi et al., 2019; Feng et al., 2020). The threat of persistent element pollution is different from the risk of organic pollutants, which may be reduced or eliminated through physical, chemical, or biological purification (Barrios-Estrada et al., 2018; Barakat et al., 2020). However, organisms can enrich these harmful elements and partially convert them into element–organic compounds with increased toxicity level (O'Donoghue et al., 2020). Arsenic (As) and mercury (Hg) are widely investigated typical elements due to their diverse origins (Shi et al., 2012; Duodu et al., 2017), persistence (Kyle et al., 2012; Beau et al., 2019), toxicity (Calderón et al., 2001; Flanders et al., 2019), and bioaccumulation performance (Greani et al., 2017; Kershaw and Hall, 2019). Hence, pollution caused by As and Hg has attracted considerable attention from researchers worldwide (Zhao et al., 2015; Maage et al., 2017; Day et al., 2019; Nyanza et al., 2020).

As and Hg released to the environment may be transported to coastal and marine regions through rainfall, surface runoffs, and atmospheric pathways (Jafarabadi et al., 2017). As an important material cycling node, surface sediments play a vital role in the sorption and transport of As and Hg in aquatic environments (Bloom et al., 1999; Furtado et al., 2019). This study investigates As and Hg in sediments from the Changjiang River Estuary and adjacent East China Sea. The mainland region adjacent to the present study area is a developed area in China. Although

sources of As and Hg in the ocean are varied, the release of upper and local streams in these water systems serves as a major mass transport (Li et al., 2014; Liu et al., 2016). For instance, up to around 2 000 t of As was directly discharged to the East China Sea by the Changjiang River alone in 2015 (<http://www.nmdis.org.cn/hygb/zggyhjzlg/>). Therefore, As and Hg should be investigated in the comprehensive environmental evaluation of these regions.

Atomic fluorescence spectrometry is commonly used in detecting As and Hg in environmental samples. However, the universal phenomena of heavy target losses, poor repeatability, and low recovery in long-term analysis still need to be solved. Therefore, the present study proposes an optimized atomic fluorescence spectrometry that includes an optimized pretreatment procedure for the determination of As and Hg in sediments. The proposed method is validated in terms of recovery, precision, and limit of quantification (LOQ).

The occurrence of As and Hg in surface sediments of the Changjiang River Estuary and adjacent East China Sea is examined using the optimized method. Moreover, a preliminary environmental risk assessment is performed to explore the environmental hazards of As and Hg pollution along the coast of Changjiang River Estuary and adjacent East China Sea.

2 Materials and methods

2.1 Study area and sampling

Samples used in this study were gathered from the Changjiang River Estuary (March 2015, $n = 27$) and the contiguous zone

of East China Sea (June 2015, $n = 11$) (Fig. 1). The Changjiang River, Qiantang River, Oujiang River, and Minjiang River flow into these coastal areas. The Yellow Sea Coastal Current, Zhejiang-Fujian Coastal Current, Taiwan Warm Current, and Kuroshio Current constitute shelf circulation in the investigated waters (Liu et al., 2007).

Samples were collected from the top 2 cm of sediment using the box grab method, stored in polyethylene sealed packets, and frozen at -20°C prior to the experiment. Crystallite dimensions of samples were measured using a laser particle analyzer (BT-9300ST, Bettersize Instruments Ltd.) with a range and mean of 0.7–189 μm and 31.6 μm , respectively. Fine-grained samples were generally dispersed in the interior estuary and near-shore area. Sediments gradually coarsened and the mean sediment crystallite dimension increased from the near-shore area to the seaward direction.

2.2 Chemical analysis

A series of standard solutions was prepared to determine standard calibration curves. Solution concentrations were 0 $\mu\text{g/L}$, 0.500 $\mu\text{g/L}$, 1.000 $\mu\text{g/L}$, 2.000 $\mu\text{g/L}$, 4.000 $\mu\text{g/L}$, 8.000 $\mu\text{g/L}$, and 16.000 $\mu\text{g/L}$ for As and 0 $\mu\text{g/L}$, 0.040 $\mu\text{g/L}$, 0.080 $\mu\text{g/L}$, 0.160 $\mu\text{g/L}$, 0.320 $\mu\text{g/L}$, 0.400 $\mu\text{g/L}$, and 0.640 $\mu\text{g/L}$ for Hg.

Prior to analyzing heavy metal (HM) contents, sediment samples were air-dried in the laboratory, homogenized using an agate mortar, and filtered through a sieve with a mesh size of 180 μm . Powdered dry samples (0.3000 g) were completely digested in airtight Teflon containers. This study optimized the sample digestion process. Figure 2 presents the detailed information of the procedure. In summary, different digestive solution systems were

compared during the pretreatment process, and the temperature of the digestion environment and solution volume were also investigated. As and Hg contents in digestive solutions were determined using an atomic fluorescence spectrometer (AFS-933, Beijing Jitian Instruments Co., Ltd.).

2.3 Quality assurance and quality control

Laboratory vessels were pre-cleaned with nitric acid and ultrapure water to prevent unintended contamination. Parallel specimens were collected in each of the 10 stations. Procedural blanks were subjected to the entire testing process. LOQ was determined using the signal-to-noise ratio of 10:1 in analytes. Method accuracy and precision were tested using recovery (RE) at two concentration levels (0.500–8.000 $\mu\text{g/L}$ for As and 0.040–400 $\mu\text{g/L}$ for Hg) by spiking sediment samples with native analytes at the beginning of the preparation procedure. Precision was likewise determined via the standard deviation (SD) of the 10 replicate analyses of the same sample. The information on method performance is listed in Table 1.

3 Results and discussion

3.1 Comparison of different digestion processes

Six types of digestive solution systems, namely, HCl-HNO₃-HF, HNO₃-HF-HClO₄, HNO₃-HF-H₂SO₄, aqua regia, aqua regia-H₂O, and HNO₃-H₂O₂, were analyzed according to actual working conditions and denoted 1 to 6. The recovery rate and SD of different digestive solution systems are illustrated in Fig. 3.

Traditional methods of elemental analyses typically use the digestive solution systems of HCl-HNO₃-HF (Tüzen, 2003; Mali

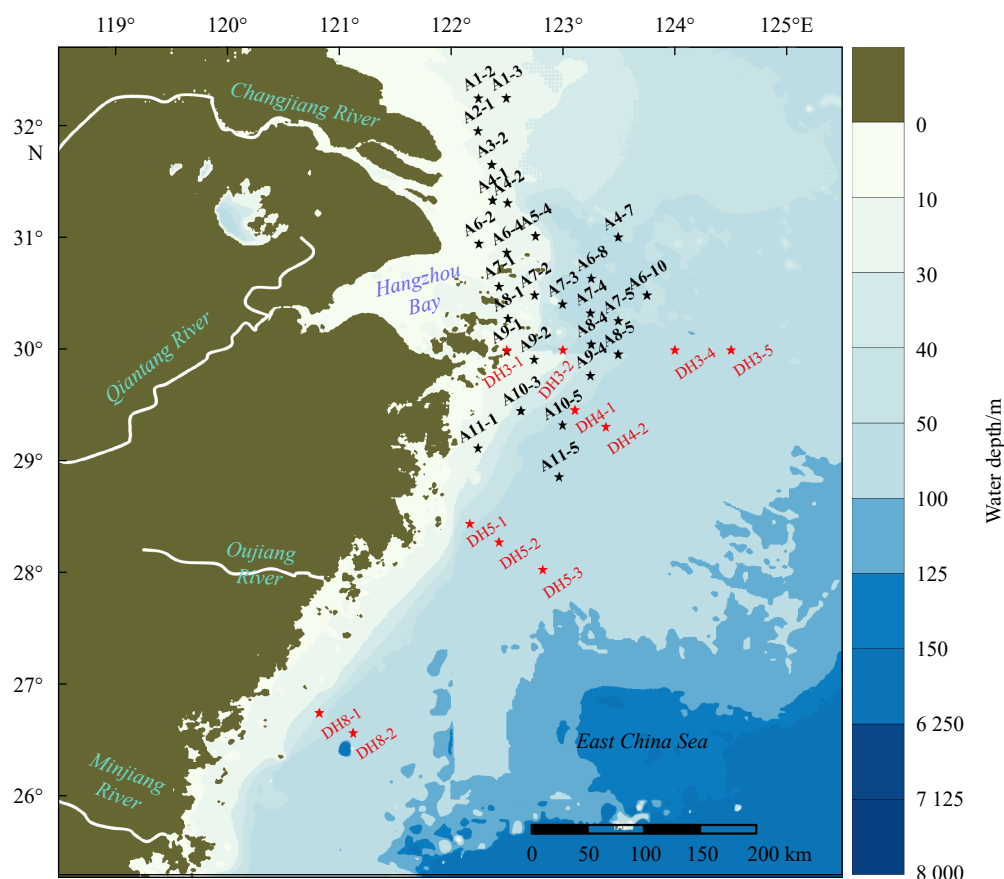


Fig. 1. Sampling locations of the Changjiang River Estuary (black star) and adjacent East China Sea (red star).

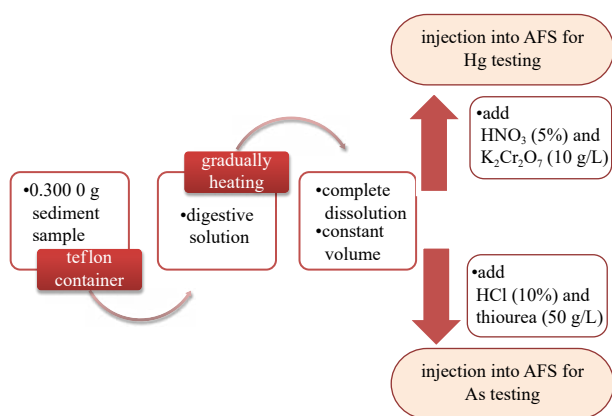


Fig. 2. Detailed information on the digestion procedure. AFS is atomic fluorescence spectrometer.

et al., 2017) and $\text{HNO}_3\text{-HF-HClO}_4$ (Zhao et al., 2016; Ravankhah et al., 2017). On the basis of our experimental results, highly acidic mixed environments with mean recoveries between 89% and 94% were significantly effective in As digestion. However, Hg di-

gestion with mean recoveries between 82% and 85% was unsatisfactory in these environments. H_2SO_4 was also used to replace HCl or HClO_4 in the highly acidic system, and the results were worse than the findings of previous systems. Furthermore, the $\text{HNO}_3\text{-H}_2\text{O}_2$ system typically used in plant sample digestion (Fang et al., 2016) was also investigated. The results in the digestion of sediments were worse than the findings of highly acidic systems. Mean recoveries of As and Hg were only 57% and 47%, respectively. Liu and Luo (2018) simultaneously determined As and Hg in soils, and aqua regia was utilized in the sample pretreatment; this method demonstrated excellent accuracy and stability. Accordingly, we attempted to use aqua regia in marine sediment preparations. The introduction of aqua regia clearly enhanced the digestive efficiency, particularly in Hg (recovery was nearly 99%). A mixture of 1:1 aqua regia- H_2O was used as the optimal digestive system to save the reagent and protect the environment. Similar to the recovery and stability of the pure aqua regia system, this system obtained excellent results. Furthermore, the introduction of aqua regia can effectively prevent the production of acid fog during the pretreatment process and consequently protect the laboratory environment and experimenter. Therefore, the aqua regia- H_2O system exhibits more benefits compared with other systems.

Table 1. Information on method performance in the investigated matrices ($n=10$)

Element	Concentration level	Linear range/ $(\mu\text{g}\cdot\text{g}^{-1})$	R^2	LOQ/ $(\mu\text{g}\cdot\text{g}^{-1})$	(Recovery \pm SD)/%	RSD/%
As	high	0–25	0.999 4	0.020	97.36 ± 2.90	3.00
	low	0–25	0.999 4	0.020	97.56 ± 4.00	4.12
Hg	high	0–1	0.999 9	0.010	98.81 ± 2.70	2.69
	low	0–1	0.999 9	0.010	98.25 ± 3.20	3.29

Note: LOQ is limit of quantification; SD is standard deviation; RSD is relative standard deviation.

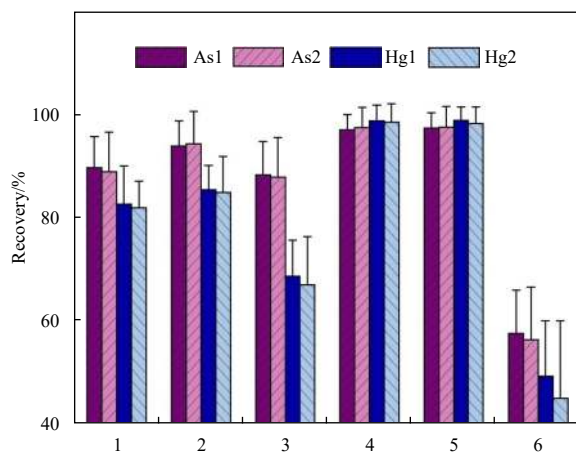


Fig. 3. Recovery rate and SD of different digestive solution systems. Codes 1 to 6 represent the different digestive solution systems of $\text{HCl-HNO}_3\text{-HF}$, $\text{HNO}_3\text{-HF-HClO}_4$, $\text{HNO}_3\text{-HF-H}_2\text{SO}_4$, aqua regia, aqua regia- H_2O , and $\text{HNO}_3\text{-H}_2\text{O}_2$. As1 and Hg1 represent high concentration, As2 and Hg2 represent low concentration.

3.2 Preprocessing and method performance

Years of actual work experiences have determined the following operational warnings. First, placing weighed samples in digestive solutions overnight was an important step in efficiently achieving complete digestion. Second, the lid of the digestion tube should be removed at the beginning of temperature programming to prevent liquid flooding. Third, shaking the diges-

tion tube was an essential step during digestion. Fourth, adding reductants into the digestive solution maintained As in its reduced form (As^{3+}). Fifth, thiourea was used as the reductant in this study. In particular, we compared the reduction of thiourea and ascorbic acid, and found no remarkable difference in the results.

Under optimized process conditions, LOQ was $0.020 \mu\text{g/g}$ and $0.010 \mu\text{g/g}$ for As and Hg, respectively. Recoveries of As and Hg were 97.36% and 98.81% in high concentrations and 97.56% and 98.25% in low concentrations, respectively. Relative SD was in the range of 3.00%–4.12% for As and 2.69%–3.29% for Hg (Table 1). These findings verified the credibility, stability, and excellent advantage of the proposed method. Thus, the proposed method can satisfy the requirements of accurate quantification of As and Hg in marine sediments.

3.3 As and Hg in sediments from the Changjiang River Estuary and adjacent East China Sea

Table 2 and Fig. 4 depict the contents of As and Hg in sediments of the Changjiang River Estuary and adjacent East China Sea. The range of content values was 2.39–8.77 $\mu\text{g/g}$ for As and 48.03–410.8 ng/g for Hg. The data show that the increase in distance from mainland areas gradually reduces the contents of As and Hg in samples, with high content in coastal sites. High contents of As were typically located in coastal areas near mainland regions, particularly in the estuary areas of Changjiang River and Qiantang River. Hg content was also high in estuary areas, with the maximum Hg contents were observed in the Zhejiang Coast. The results indicated that an inverse correlation existed between As and Hg contents and crystallite dimensions. The data were consistent with the results of previous studies, such as that the

Table 2. Distribution and geoaccumulation index in 38 sediment samples of this study

Site	Content		TOC/%	Grain size/ μm	I_{geo}		Site	Content		TOC/%	Grain size/ μm	I_{geo}	
	As/ $(\mu\text{g}\cdot\text{g}^{-1})$	Hg/ $(\text{ng}\cdot\text{g}^{-1})$			As	Hg		As/ $(\mu\text{g}\cdot\text{g}^{-1})$	Hg/ $(\text{ng}\cdot\text{g}^{-1})$			As	Hg
DH3-1	7.44	120.0	0.847	11.02	0.09	0.77	A6-4	7.32	288.9	0.765	9.89	0.07	2.03
DH3-2	4.26	125.9	0.783	5.70	-0.71	0.83	A6-8	2.96	203.0	0.742	86.47	-1.24	1.52
DH3-4	2.64	48.03	0.532	12.90	-1.40	-0.56	A6-10	2.72	119.7	0.626	10.19	-1.36	0.76
DH3-5	2.39	62.13	0.362	189.20	-1.54	-0.18	A7-1	8.59	301.1	0.852	10.25	0.30	2.09
DH4-1	4.18	89.07	0.718	10.25	-0.74	0.34	A7-2	8.14	295.3	0.779	17.43	0.22	2.06
DH4-2	3.08	77.42	0.824	33.50	-1.18	0.13	A7-3	5.85	218.7	0.753	22.68	-0.25	1.63
DH5-1	7.67	309.1	0.701	3.67	0.14	2.13	A7-4	3.65	161.3	0.725	9.69	-0.93	1.19
DH5-2	6.64	132.3	0.589	6.12	-0.07	0.91	A7-5	3.25	194.2	0.660	94.88	-1.10	1.46
DH5-3	3.40	76.92	0.456	120.50	-1.04	0.12	A8-1	8.77	296.1	0.881	8.77	0.33	2.07
DH8-1	7.36	151.6	0.798	22.65	0.08	1.10	A8-4	3.41	173.5	0.705	12.61	-1.03	1.30
DH8-2	4.85	101.7	0.749	11.54	-0.52	0.53	A8-5	3.28	208.1	0.660	7.04	-1.09	1.56
A1-2	5.53	247.9	0.751	84.24	-0.33	1.81	A9-1	6.11	142.4	0.871	29.29	-0.19	1.01
A1-3	5.99	200.8	0.626	100.70	-0.22	1.51	A9-2	7.12	267.1	0.837	8.53	0.03	1.92
A2-1	6.98	298.5	0.768	10.44	0.00	2.08	A9-4	3.43	197.6	0.716	14.39	-1.02	1.49
A3-2	7.23	164.6	0.747	9.31	0.05	1.22	A10-3	7.26	410.8	0.849	0.66	0.06	2.54
A4-1	8.39	201.7	0.793	12.88	0.27	1.51	A10-5	4.91	193.2	0.781	7.81	-0.50	1.45
A4-2	6.48	173.9	0.770	6.88	-0.10	1.30	A11-1	8.66	372.7	0.880	4.37	0.31	2.40
A4-7	2.60	54.26	0.647	111.30	-1.42	-0.38	A11-5	5.32	273.6	0.759	42.45	-0.39	1.95
A5-4	6.49	209.7	0.739	26.51	-0.10	1.57	Min	2.39	48.03	0.362	0.66	-1.54	-0.56
A6-2	7.92	208.7	0.787	15.06	0.18	1.56	max	8.77	410.8	0.881	189.20	0.33	2.54

Note: TOC is total organic carbon.

small particle size of sediments increased the adsorption capacity of HMs (Spagnoli and Andresini, 2018). This condition may be explained by the large specific surface area due to the small particle size of sediments that increased the amount of equilibrium adsorption of HMs. Total organic carbon (TOC) contents of sediments were also analyzed, on account of the correlation between HM distributions and TOC contents to some extent. A phenomenon in which As and Hg contents levels had positive correlation with TOC contents was consistent with the previous study (Alshemmari and Talebi, 2019). This observation might be related to the great affinity and numerous polar functional groups of organic matter. According to the principal component analysis, TOC contents exerted a weaker influence on element distribution patterns compared with sediment crystallite dimensions in this study. In addition, distribution characters of elements validated that As and Hg in this area were partially affected by terrigenous input in this study. A survey demonstrated that HMs (copper, plumbum, zinc, cadmium, Hg, and As) draining from rivers into the East China Sea reached approximately 14.2×10^3 t in 2015 (<http://www.nmdis.org.cn/hygb/zghyhjzlgb/>). The influence of land-based pollutants caused by highly industrialized coastal regions and inputs of great rivers must be considered.

A comparison of As and Hg content levels in sediments from the investigated areas and other coastal zones in the world is presented in Table 3. The investigated areas demonstrated relatively low As content levels compared with other coastal areas of China and the rest of the world. Notably, the Hg content levels in the investigated areas were relatively higher than the results of other coastal areas in China, although these findings were lower than the Hg content levels of other coastal areas in the world. This finding is likely due to the serious Hg pollution in the study area or the relatively high detection contents obtained by the optimized analysis method. In addition, the ecological environment of As and Hg in the investigated sea area demonstrated a significant improvement in recent years compared with the res-

ults of previous studies likely due to the recently increased environmental protection efforts in China.

3.4 Ecological risk assessment of As and Hg

The geoaccumulation index (I_{geo}) was used in the preliminary ecological risk assessment (Table 2 and Fig. 5). I_{geo} quantitatively evaluated the degree of HM contamination while synthetically considering human activities and natural geological processes (Müller, 1979). This index is frequently used in the assessment of HM enrichment in sediments as follows:

$$I_{\text{geo}} = \log_2 \left(\frac{C_i}{kB_i} \right), \quad (1)$$

where C_i is the measured content of examined metal i ; B_i is the background content of metal i ; and factor k ($k = 1.5$) is introduced as the possible variation in background values due to anthropogenic influences or lithologic variations. On the basis of the synthesis method of a previous study on soil geochemical baselines of eastern coastal China (Yan et al., 1997; Chen et al., 2008), background contents of target elements were $9.29 \mu\text{g/g}$ and $0.040 \mu\text{g/g}$ for As and Hg, respectively. According to the increasing values, I_{geo} assesses the degree of metal pollution in terms of seven classes to express different contamination levels ranging from nearly unpolluted to extremely polluted (Förstner et al., 1990).

I_{geo} values of As and Hg in the investigated samples were in the range of -1.54 to 0.33 and -0.56 to 2.54 , respectively. Two-thirds of the I_{geo} values of As were less than 0. This finding indicated that samples were practically unpolluted according to the I_{geo} classification (Müller, 1979). The remaining one-third of the I_{geo} values of As were between 0 and 1. Thus, several stations of the study area exhibited a slight enrichment level. Overall, As posed a minimal threat to the study area. By comparison, the I_{geo} values of Hg implied a serious pollution situation. Only 8% of the

I_{geo} values of Hg was less than 0% and 71% was more than 1. These findings indicated moderate to heavy pollution in the

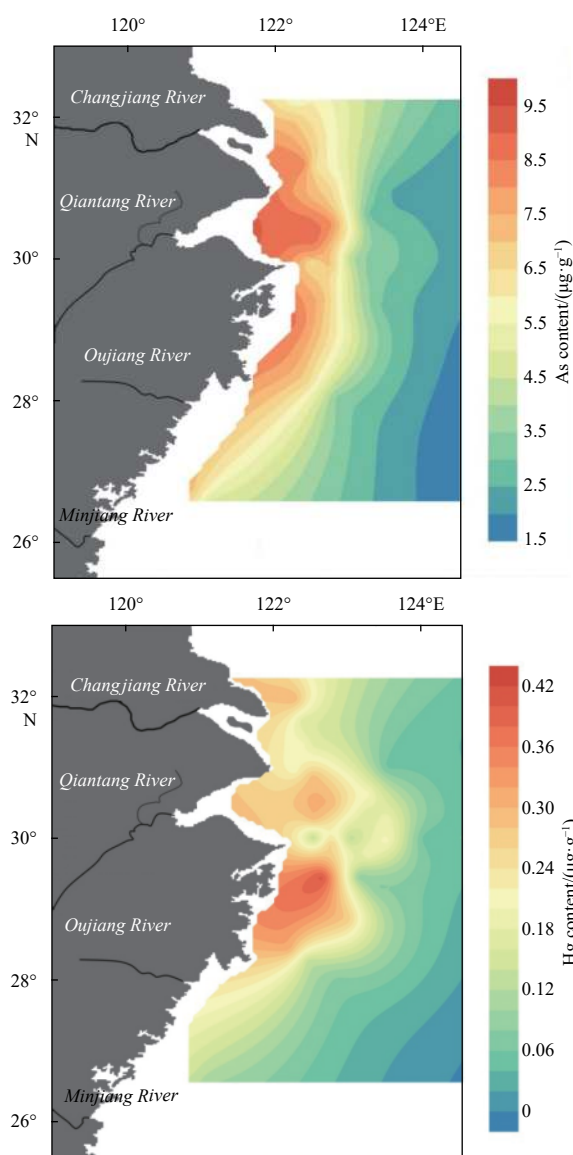


Fig. 4. Distributions of As and Hg contents in the surface sediments from the Changjiang River Estuary and adjacent East China Sea during the study.

study area. The dominant position of HMs in the samples from weathering detrital in the downstream and estuary of Changjiang River was consistent with the findings of previous investigations (Zhang et al., 1990).

The following anthropogenic contribution rate proposed by N'guessan et al. (2009) based on the calculation model of enrichment factor is used in this study to exclude anthropogenic activities from the natural background and reflect the contribution of human activities to As and Hg distribution in sediments of the study area quantitatively:

$$M = \frac{C_{\text{sample}} - X_{\text{sample}} \times (C_{\text{baseline}}/X_{\text{baseline}})}{C_{\text{sample}}} \times 100\%, \quad (2)$$

where M is the anthropogenic contribution rate, C is the target HM, and X is the reference element primarily combined with silicate minerals (Lee et al., 1994). Aluminum was selected as the reference element to calculate M in this study.

The analysis showed that M values of As in the investigated samples ranged from 0% to 50%, with an average value of 22%. This result verified that As in the investigated sediments are slightly influenced by artificiality and primarily originate from natural weathering processes. However, anthropogenic contribution rates of Hg ranged from 4% to 91%, with an average value of 72%. The majority of M values of Hg at more than 50% indicated the clear effects of anthropogenic contribution on the Hg distribution in sediments from the study area.

Anthropogenic activities caused by the rapid economy development have enriched Hg and other HMs in the past (He et al., 2019a). However, the Chinese government has made notable efforts on environmental protection. The survey showed that pollutant emissions are effectively controlled with the active economy. By taking the mass control of contaminants carried by the Changjiang River as an example, the pollutions of As and five kinds of HMs, including Hg, zinc, copper, lead, and cadmium, have been significantly reduced in recent years (Fig. 6, <http://www.nmdis.org.cn/hygb/zghyhjzlg/>). Fan et al. (2019) and Li et al. (2019) also confirmed that the quality of ecological environment of this sea area demonstrated a trend of fluctuating improvement over time, especially after 2015, after a long period of macrocontrol against environment protection.

4 Conclusions

An effective procedure for the simultaneous determination of As and Hg in marine sediment samples was established in this

Table 3. Comparisons of As and Hg levels in the sediments of the Changjiang River Estuary, the adjacent East China Sea and the other coastal zones in the world

Location	As content/($\mu\text{g}\cdot\text{g}^{-1}$)	Hg content/($\mu\text{g}\cdot\text{g}^{-1}$)	Reference
Changjiang River Estuary (sampling year in 2007)	10.3	0.06	He et al. (2019b)
Changjiang River Estuary (sampling year in 2010)	14.5	0.68	Fang et al. (2013)
Changjiang River Estuary and adjacent East China Sea (sampling year in 2015)	5.59	0.19	in this study
Bohai Sea	9.18	0.04	Zhu et al. (2019)
Yellow Sea	ND–18.17	ND–0.13	Shen et al. (2018)
The west of Guangdong coastal region, China	20.8	0.13	Zhao et al. (2016)
The Apulia region	9.10	0.24	Mali et al. (2017)
Coastal area of District Badin	–	0.20	Qureshi et al. (2015)
Ambarlı Port area, Sea of Marmara	–	0.13	Sarı et al. (2013)
Izmir Bay, Eastern Aegean Sea	16.1	–	Gonul (2015)
Baltic Sea	5.1–17.0	–	Bełdowski et al. (2016)

Note: ND represents non-detected, – represents no data.

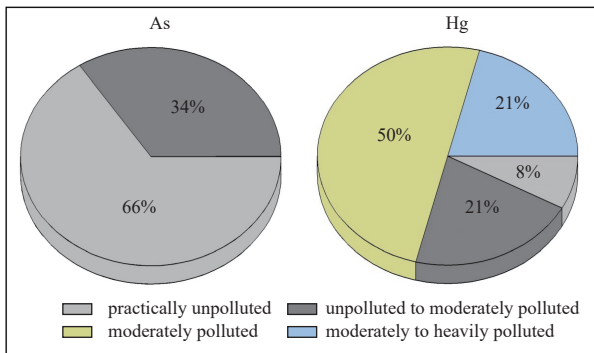


Fig. 5. Geoaccumulation index (I_{geo}) gradations of As and Hg in all the sampling sites.

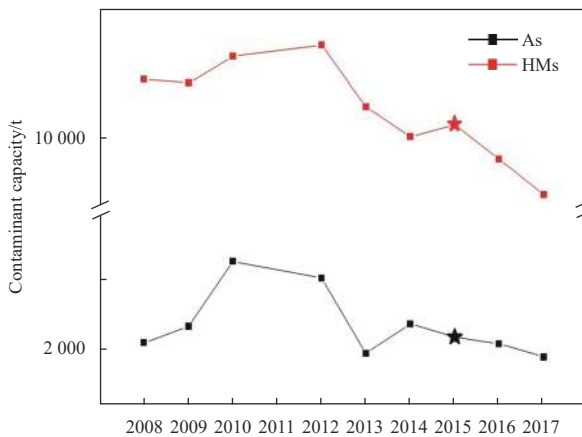


Fig. 6. Capacity of total (dissolved and particulate) As and HMs carried by the Changjiang River from 2007 to 2018 (the symbol star represents sampling year of this study).

study. The aqua regia–H₂O system was used as the pretreatment procedure for sample digestion and certain operational warnings were optimized. The results indicated that the proposed method performs better than previously reported approaches and can be used in the accurate quantification of As and Hg in marine sediments. Under optimum process conditions, As and Hg obtained LOQs of 0.020 µg/g and 0.010 µg/g and recoveries of 97% and 98%, respectively, with suitable precisions (2.69%–4.12%).

The proposed method was used in the quantitative analysis of As and Hg in surface sediment samples collected from the Changjiang River Estuary (March 2015, $n = 27$) and the adjacent East China Sea (June 2015, $n = 11$). The results revealed that As and Hg were abundant in the investigated samples. The range of content values was 2.39–8.77 µg/g for As and 48.03–410.8 ng/g for Hg. The gradually decreasing As and Hg contents with increasing distance from mainland areas indicated that spatial distributions of As and Hg in the study area are strongly influenced by terrigenous input. I_{geo} and M were applied in the preliminary ecological risk assessment. Despite significant improvement in China's environment, the strong ecological risk demonstrated by Hg in sediments from the Changjiang River Estuary and the adjacent East China Sea must be investigated further.

Acknowledgements

We are very grateful to Guipeng Yang from Ocean University

of China for his technical assistance. Meanwhile, we are grateful to the captain and crew of the R/V *Runjiang No.1* for help and co-operation during the cruise.

References

- Alshemmari H, Talebi L. 2019. Heavy metal concentrations in the surface sediments of the northwestern Arabian Gulf, Kuwait. *Arabian Journal of Geosciences*, 12(18): 565, doi: [10.1007/s12517-019-4751-z](https://doi.org/10.1007/s12517-019-4751-z)
- Awasthi A K, Wang Mengmeng, Awasthi M K, et al. 2018. Environmental pollution and human body burden from improper recycling of e-waste in China: a short-review. *Environmental Pollution*, 243: 1310–1316, doi: [10.1016/j.envpol.2018.08.037](https://doi.org/10.1016/j.envpol.2018.08.037)
- Barakat M A, Anjum M, Kumar R, et al. 2020. Design of ternary Ni(OH)₂/graphene oxide/TiO₂ nanocomposite for enhanced photocatalytic degradation of organic, microbial contaminants, and aerobic digestion of dairy wastewater. *Journal of Cleaner Production*, 258: 120588, doi: [10.1016/j.jclepro.2020.120588](https://doi.org/10.1016/j.jclepro.2020.120588)
- Barrios-Estrada C, de Jesús Rostro-Alanis M, Muñoz-Gutiérrez B D, et al. 2018. Emergent contaminants: endocrine disruptors and their laccase-assisted degradation—A review. *Science of the Total Environment*, 612: 1516–1531, doi: [10.1016/j.scitotenv.2017.09.013](https://doi.org/10.1016/j.scitotenv.2017.09.013)
- Beau F, Bustamante P, Michaud B, et al. 2019. Environmental causes and reproductive correlates of mercury contamination in European pond turtles (*Emys orbicularis*). *Environmental Research*, 172: 338–344, doi: [10.1016/j.envres.2019.01.043](https://doi.org/10.1016/j.envres.2019.01.043)
- Beldowski J, Szubska M, Emelyanov E, et al. 2016. Arsenic concentrations in Baltic Sea sediments close to chemical munitions dumpsites. *Deep Sea Research Part II: Topical Studies in Oceanography*, 128: 114–122, doi: [10.1016/j.dsr2.2015.03.001](https://doi.org/10.1016/j.dsr2.2015.03.001)
- Bloom N S, Gill G A, Cappellino S, et al. 1999. Speciation and cycling of mercury in Lavaca Bay, Texas, sediments. *Environmental Science & Technology*, 33(1): 7–13
- Calderón J, Navarro M E, Jimenez-Capdeville M E, et al. 2001. Exposure to arsenic and lead and neuropsychological development in Mexican children. *Environmental Research*, 85(2): 69–76, doi: [10.1006/enrs.2000.4106](https://doi.org/10.1006/enrs.2000.4106)
- Chen Guoguang, Xi Xiaohuan, Liang Xiaohong, et al. 2008. Soil geochemical baselines of the Yangtze River delta and their significances. *Geoscience (in Chinese)*, 22(6): 1041–1048
- Day P L, Nelson E J, Bluhm A M, et al. 2019. Discovery of an arsenic and mercury co-elevation in the Midwest United States using reference laboratory data. *Environmental Pollution*, 254: 113049, doi: [10.1016/j.envpol.2019.113049](https://doi.org/10.1016/j.envpol.2019.113049)
- Duodu G O, Goonetilleke A, Ayoko G A. 2017. Potential bioavailability assessment, source apportionment and ecological risk of heavy metals in the sediment of Brisbane River estuary, Australia. *Marine Pollution Bulletin*, 117(1–2): 523–531
- Fan Haimei, Jiang Xiaoshan, Ji Huanhong, et al. 2019. Integrated evaluation of the marine ecological environment in the Yangtze River Estuary and its adjacent area. *Acta Ecologica Sinica (in Chinese)*, 39(13): 4660–4675
- Fang Yong, Pan Yushi, Li Peng, et al. 2016. Simultaneous determination of arsenic and mercury species in rice by ion-pairing reversed phase chromatography with inductively coupled plasma mass spectrometry. *Food Chemistry*, 213: 609–615, doi: [10.1016/j.foodchem.2016.07.003](https://doi.org/10.1016/j.foodchem.2016.07.003)
- Fang Ming, Wu Youjun, Liu Hong, et al. 2013. Distribution, sources and ecological risk assessment of heavy metals in sediments of the Yangtze River estuary. *Acta Scientiae Circumstantiae (in Chinese)*, 33(2): 563–569
- Feng Zhihua, Zhang Tao, Wang Jiakuan, et al. 2020. Spatio-temporal features of microplastics pollution in macroalgae growing in an important mariculture area, China. *Science of the Total Environment*, 719: 137490, doi: [10.1016/j.scitotenv.2020.137490](https://doi.org/10.1016/j.scitotenv.2020.137490)
- Flanders J, Long G, Reese B, et al. 2019. Assessment of potential mercury toxicity to native invertebrates in a high-gradient stream. *Integrated Environmental Assessment and Management*, 15(3): 374–384, doi: [10.1002/ieam.4133](https://doi.org/10.1002/ieam.4133)
- Förstner U, Ahlf W, Calmano W, et al. 1990. Sediment criteria development: contributions from environmental geochemistry to

- water quality management. In: Heling D, Rothe P, Förstner U, et al., eds. *Sediments and Environmental Geochemistry*. Berlin, Heidelberg: Springer, 311–338
- Furtado R, Pereira M E, Granadeiro J P, et al. 2019. Body feather mercury and arsenic concentrations in five species of seabirds from the Falkland Islands. *Marine Pollution Bulletin*, 149: 110574, doi: [10.1016/j.marpolbul.2019.110574](https://doi.org/10.1016/j.marpolbul.2019.110574)
- Gonul L T. 2015. Chemical speciation and ecological risk assessment of arsenic in marine sediments from Izmir Bay (Eastern Aegean Sea). *Environmental Science and Pollution Research*, 22(24): 19951–19960, doi: [10.1007/s11356-015-5197-9](https://doi.org/10.1007/s11356-015-5197-9)
- Greani S, Lourkisti R, Berti L, et al. 2017. Effect of chronic arsenic exposure under environmental conditions on bioaccumulation, oxidative stress, and antioxidant enzymatic defenses in wild trout *Salmo trutta* (Pisces, Teleostei). *Ecotoxicology*, 26(7): 930–941, doi: [10.1007/s10646-017-1822-3](https://doi.org/10.1007/s10646-017-1822-3)
- He Zhongfa, Li Fangliang, Dominech S, et al. 2019a. Heavy metals of surface sediments in the Changjiang (Yangtze River) Estuary: distribution, speciation and environmental risks. *Journal of Geochemical Exploration*, 198: 18–28, doi: [10.1016/j.gexplo.2018.12.015](https://doi.org/10.1016/j.gexplo.2018.12.015)
- He Zhongfa, Yang Shouye, Zhao Baocheng, et al. 2019b. Changes in heavy metal elements in the sediments from Changjiang Estuary and their environmental responses in recent 1 500 years. *Marine Geology & Quaternary Geology (in Chinese)*, 39(2): 21–30
- Jafarabadi A R, Bakhtiyari A R, Toosi A S, et al. 2017. Spatial distribution, ecological and health risk assessment of heavy metals in marine surface sediments and coastal seawaters of fringing coral reefs of the Persian Gulf, Iran. *Chemosphere*, 185: 1090–1111, doi: [10.1016/j.chemosphere.2017.07.110](https://doi.org/10.1016/j.chemosphere.2017.07.110)
- Kershaw J L, Hall A J. 2019. Mercury in cetaceans: exposure, bioaccumulation and toxicity. *Science of the Total Environment*, 694: 133683, doi: [10.1016/j.scitotenv.2019.133683](https://doi.org/10.1016/j.scitotenv.2019.133683)
- Kyle J H, Breuer P L, Bunney K G, et al. 2012. Review of trace toxic elements (Pb, Cd, Hg, As, Sb, Bi, Se, Te) and their deportment in gold processing: Part II. deportment in gold ore processing by cyanidation. *Hydrometallurgy*, 111–112: 10–21
- Lee D S, Garland J A, Fox A A. 1994. Atmospheric concentrations of trace elements in urban areas of the United Kingdom. *Atmospheric Environment*, 28(16): 2691–2713, doi: [10.1016/1352-2310\(94\)90442-1](https://doi.org/10.1016/1352-2310(94)90442-1)
- Li Lei, Jiang Mei, Liu Yong, et al. 2019. Heavy metals inter-annual variability and distribution in the Yangtze River estuary sediment, China. *Marine Pollution Bulletin*, 141: 514–520, doi: [10.1016/j.marpolbul.2019.03.008](https://doi.org/10.1016/j.marpolbul.2019.03.008)
- Li Lei, Ren Jingling, Yan Zhe, et al. 2014. Behavior of arsenic in the coastal area of the Changjiang (Yangtze River) Estuary: influences of water mass mixing, the spring bloom and hypoxia. *Continental Shelf Research*, 80: 67–78, doi: [10.1016/j.csr.2014.02.021](https://doi.org/10.1016/j.csr.2014.02.021)
- Liu Maodian, Chen Long, Wang Xuejun, et al. 2016. Mercury export from mainland China to adjacent seas and its influence on the marine mercury balance. *Environmental Science & Technology*, 50(12): 6224–6232
- Liu Jinglong, Luo Shoujuan. 2018. Simultaneous Determination of arsenic and mercury in soil by atomic fluorescence spectrometry with the samples dissolved in aqua regia. *Environmental Science Survey (in Chinese)*, 37(5): 88–90
- Liu J P, Xu K H, Li A C, et al. 2007. Flux and fate of Yangtze River sediment delivered to the East China Sea. *Geomorphology*, 85(3–4): 208–224
- Maage A, Nilsen B M, Julshamn K, et al. 2017. Total mercury, methylmercury, inorganic arsenic and other elements in meat from minke whale (*Balaenoptera acutorostrata*) from the north east Atlantic Ocean. *Bulletin of Environmental Contamination and Toxicology*, 99(2): 161–166, doi: [10.1007/s00128-017-2106-6](https://doi.org/10.1007/s00128-017-2106-6)
- Mali M, Dell'Anna M M, Mastorilli P, et al. 2017. Assessment and source identification of pollution risk for touristic ports: heavy metals and polycyclic aromatic hydrocarbons in sediments of 4 marinas of the Apulia region (Italy). *Marine Pollution Bulletin*, 114(2): 768–777, doi: [10.1016/j.marpolbul.2016.10.063](https://doi.org/10.1016/j.marpolbul.2016.10.063)
- Müller G. 1979. Heavy metals in the sediment of the Rhine-changes seity. *Umschau in Wissenschaft und Technik*, 79: 778–783
- N'guessan Y M, Probst J L, Bur T, et al. 2009. Trace elements in stream bed sediments from agricultural catchments (Gascogne region, S-W France): where do they come from?. *Science of the Total Environment*, 407(8): 2939–2952, doi: [10.1016/j.scitotenv.2008.12.047](https://doi.org/10.1016/j.scitotenv.2008.12.047)
- Nyanza E C, Dewey D, Manyama M, et al. 2020. Maternal exposure to arsenic and mercury and associated risk of adverse birth outcomes in small-scale gold mining communities in Northern Tanzania. *Environment International*, 137: 105450, doi: [10.1016/j.envint.2019.105450](https://doi.org/10.1016/j.envint.2019.105450)
- O'Donoghue J L, Watson G E, Brewer R, et al. 2020. Neuropathology associated with exposure to different concentrations and species of mercury: a review of autopsy cases and the literature. *Neurotoxicology*, 78: 88–98, doi: [10.1016/j.neuro.2020.02.011](https://doi.org/10.1016/j.neuro.2020.02.011)
- Qureshi M A, Mastoi G M, Baloch M A, et al. 2015. Arc GIS based interpretation of surface sediment heavy metals near coastal area of District Badin, Sindh, Pakistan. *American Journal of Environmental Protection*, 4(3): 110–119, doi: [10.11648/j.ajep.20150403.11](https://doi.org/10.11648/j.ajep.20150403.11)
- Ravankhah N, Mirzaei R, Masoum S. 2017. Determination of heavy metals in surface soils around the brick kilns in an arid region, Iran. *Journal of Geochemical Exploration*, 176: 91–99, doi: [10.1016/j.gexplo.2016.01.005](https://doi.org/10.1016/j.gexplo.2016.01.005)
- Sarı E, Ünlü S, Apak R, et al. 2013. Mercury distribution in the sediments of Ambarlı Port Area, Sea of Marmara (Turkey). *Chemistry and Ecology*, 29(1): 28–43, doi: [10.1080/02757540.2012.696614](https://doi.org/10.1080/02757540.2012.696614)
- Shen Fang, Mao Longjiang, Deng Xiaoqian, et al. 2018. Reanalysis of distribution characteristics and contamination evaluation of heavy metals in coastal sediments of Jiangsu Province. *Journal of Capital Normal University: Natural Sciences Edition (in Chinese)*, 39(5): 62–71
- Shi G, Chen Z, Teng J, et al. 2012. Fluxes, variability and sources of cadmium, lead, arsenic and mercury in dry atmospheric depositions in urban, suburban and rural areas. *Environmental Research*, 113: 28–32, doi: [10.1016/j.envres.2012.01.001](https://doi.org/10.1016/j.envres.2012.01.001)
- Shi Zhen, Wu Fengping, Huang Huinan, et al. 2019. Comparing economics, environmental pollution and health efficiency in China. *International Journal of Environmental Research and Public Health*, 16(23): 4827, doi: [10.3390/ijerph16234827](https://doi.org/10.3390/ijerph16234827)
- Spagnoli F, Andresini A. 2018. Biogeochemistry and sedimentology of Lago di Lesina (Italy). *Science of the Total Environment*, 643: 868–883, doi: [10.1016/j.scitotenv.2018.06.165](https://doi.org/10.1016/j.scitotenv.2018.06.165)
- Tützen M. 2003. Determination of heavy metals in soil, mushroom and plant samples by atomic absorption spectrometry. *Microchemical Journal*, 74(3): 289–297, doi: [10.1016/S0026-265X\(03\)00035-3](https://doi.org/10.1016/S0026-265X(03)00035-3)
- Yan Mingcai, Gu Tiexin, Chi Qinghua, et al. 1997. Abundance of chemical elements of soils in China and supergenesis geochemistry characteristics. *Geophysical and Geochemical Exploration (in Chinese)*, 21(3): 161–167
- Zhang Jing, Huang Wet Wen, Wang Qi. 1990. Concentration and partitioning of particulate trace metals in the Changjiang (Yangtze River). *Water, Air, and Soil Pollution*, 52(1–2): 57–70
- Zhao Jianru, Chu Fengyou, Jin Xianglong, et al. 2015. The spatial multiscale variability of heavy metals based on factorial kriging analysis: a case study in the northeastern Beibu Gulf. *Acta Oceanologica Sinica*, 34(12): 137–146, doi: [10.1007/s13131-015-0768-7](https://doi.org/10.1007/s13131-015-0768-7)
- Zhao Guangming, Lu Qingyuan, Ye Siyuan, et al. 2016. Assessment of heavy metal contamination in surface sediments of the west Guangdong coastal region, China. *Marine Pollution Bulletin*, 108(1–2): 268–274
- Zhu Aimei, Zhang Hui, Cui Jingjing, et al. 2019. Environmental quality assessment and influence factor of heavy metals in the surface sediments from the Bohai Sea. *Haiyang Xuebao (in Chinese)*, 41(12): 134–144